

Separation of Closely Related Structural Isomers by Inclusion Complexation with Tailor-made Host Compounds. Crystal Structures of 2,2-Di(*p*-hydroxyphenyl)propane and Its 1:1 Complex with *p*-Cresol

ISRAEL GOLDBERG* and ZAFRA STEIN

School of Chemistry, Sackler Faculty of Exact Sciences, Tel Aviv University, Ramat Aviv, 69978 Tel Aviv, Israel.

KOICHI TANAKA and FUMIO TODA*

Department of Industrial Chemistry, Faculty of Engineering, Ehime University, Matsuyama 790, Japan.

(Received: 14 February 1990; in final form: 7 June 1990)

Abstract. The crystal structures of the 2,2-di(*p*-hydroxyphenyl)propane host and its 1:1 adducts with *m*- and *p*-cresol guests have been studied. The preferential complexation of this host with *p*-cresol over *m*-cresol is related to the opposite trend exhibited by 1,1-di(*p*-hydroxyphenyl)cyclohexane; both hosts can separate effectively the two cresols from their liquid mixture by crystalline inclusion. A plausible explanation of the different inclusion features is provided by examining the intermolecular association in the corresponding solids. The analysed structures are stabilized by strong and continuous H-bonding between the constituent entities along two dimensions, and by weak van der Waals forces along the third axis. The *p*-cresol complex of the title host reveals a unique arrangement within and a more efficient packing of the layered structure, and thus represents a more stable and less soluble crystal lattice than its *m*-cresol analog.

Key words. Isomeric separations by crystalline inclusion, host design, molecular recognition of alcohols.

Supplementary Data relating to this article are deposited with the British Library as Supplementary Publication No. SUP 82099 (8 pages).

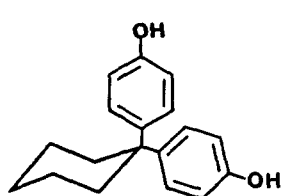
1. Introduction

Inclusion crystallization of functionalized hosts with polar guest compounds has been successfully used in recent years to separate structural isomers and to resolve optically active materials [1, 2]. Host design based on aryl alcohols as simple building blocks is exceptionally useful to this end. Suitable recent examples relate to effective enantiomeric resolutions of N-, P-, As-, S- and Se-oxides, as well as of compounds containing chiral carbon (e.g., esters of carboxylic acids, bicyclic enones and tricyclic enones), by diastereoisomeric complex formation with 2,2'-dihydroxy-1,1'-binaphthyl, 10,10'-dihydroxy-9,9'-biphenanthryl and 4,5-bis(hydroxydiphenylmethyl)-2,2-dimethyl-1,3-dioxolane [3–7]. An elegant isomeric separation of non chiral phenolic species by crystalline complexation with 1,1-di(*p*-hydroxyphenyl)-cyclohexane (1) has also been demonstrated [8]. The latter host is particularly

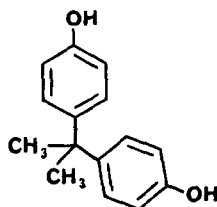
* Authors for correspondence.

selective towards *m*-cresol, allowing its efficient extraction from mixtures with *p*-cresol and other phenols, as well as from coal tar [8]. Preferential complexation of (1) with cyclohexanol from its mixture with cyclohexanone has also been reported [9]. Interpretation of the crystal structures of these complexes revealed a characteristic pattern of molecular recognition between the alcoholic species, which dominates the intermolecular arrangement in the solid state and allows discrimination against guest molecules which are sterically and functionally less compatible [8].

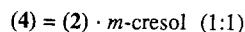
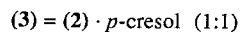
The simplicity of the host compounds enables a facile variation of their molecular structure, and a consequent modification of the selectivity features towards a given series of guest species. This can be exemplified by the inclusion behaviour of 2,2-di(*p*-hydroxyphenyl)propane (2), which is functionally very similar to diol (1) but its central alkyl part consists of the smaller and slightly more flexible propyl rather than cyclohexyl fragment. The different topology of host (2) causes, in contrast to the inclusion behaviour of (1), its preferred co-crystallization with *p*-cresol (b.p. 201.8°C) than with *m*-cresol (b.p. 202.0°C) from a mixture of the phenolic guests. This unique example of two closely related host compounds, exhibiting reversed trends of isomeric selectivity, calls for a comparative evaluation of their structural features. In this account we report on the crystal structures of the free host (2), and of its 1:1 inclusion complexes with *p*-cresol (3) and *m*-cresol (4), and relate the selectivity properties to structure. Some features of crystalline inclusion complexation of (2) with amines and hydrazines, including crystal structure determination of the 1:1 (2) · methylhydrazine adduct have already been published [10].



(1)



(2)



2. Experimental

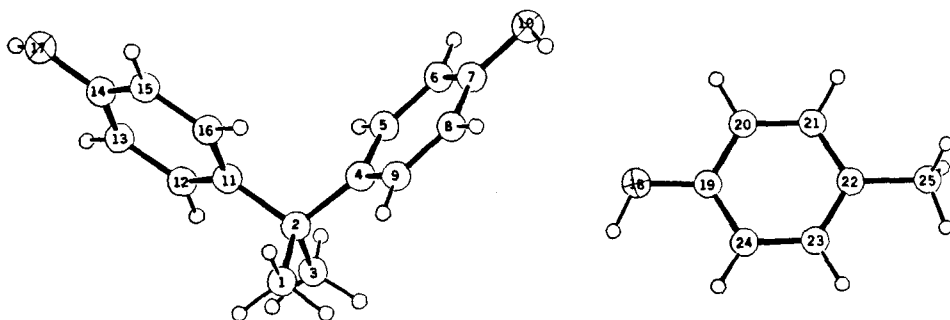
Studies of competitive crystallization followed very closely the general procedure outlined in the previous publication on complexes of the cyclohexane host derivative [8], except for using benzene instead of ethylacetate as a common solvent. Typically, equimolar amounts of two different phenols and host (2) were dissolved in benzene, and the solution was left overnight at room temperature to allow crystallization of the preferred complex. The crude form of the latter was then purified by further recrystallization from the same solvent. Finally, the guest component was recovered from the pure complex by heating at 200°C under 20 torr. With equal amounts of *p*-cresol and *m*-cresol as the competing guests, pure *p*-cresol could be isolated in the above manner in 53% yield [10].

Single crystals of the free host (m.p. 168–170°C) were obtained by slow evaporation of its solution in benzene. Crystals of the inclusion complexes (3) (m.p.

110–112°C) and (4) (m.p. 91–92°C) were prepared by mixing the corresponding pure components in benzene. The composition of the various complexes was initially verified by thermogravimetric measurements. All crystals of the inclusion compound of (2) with phenol (m.p. 94–95°C) turned out to be twinned and unsuitable for crystal structure analysis. Similar attempts to form an inclusion complex of (2) with *o*-cresol as guest were unsuccessful.

X-ray diffraction data were measured at room temperature on a CAD4 diffractometer equipped with a graphite monochromator, using MoK α ($\lambda = 0.7107 \text{ \AA}$) radiation. The crystal data and pertinent details of the experimental conditions are given in Table I. The intensities of reflections within $0 < 2\theta < 46^\circ$ were collected by the $\omega - 2\theta$ scan technique at a constant 3 deg/min rate, with a scan range of $0.9 + (0.3 \tan \theta)^\circ$. The analyzed crystals were sealed within a 0.5 mm thick Lindemann glass capillary to protect them from possible deterioration. Nevertheless, the standard reflections monitored for the inclusion crystals showed a linear decrease in their intensity as a function of time, about 10% for (3) and 18% for (4) over the entire experiment, which required an appropriate correction of the corresponding data sets. Even so, the diffraction patterns obtained for the three crystals were relatively poor, containing a large percentage of very weak reflections. The situation was particularly bad for the *m*-cresol complex where only about 25% of the measured intensities were above the background noise; correspondingly, this structure could not be fully analysed. The experimental data were converted to structure factors in a conventional manner, but were not corrected for absorption or secondary extinction.

The crystal structures of (2) and (3) were solved by direct methods (SHELXS-86) [11]. Their refinements were carried out by large-block least squares (SHELX-76) [12], including the positional and anisotropic thermal parameters of all the nonhydrogen atoms. In view of the low data-to-parameters ratio in (2) the phenyl rings of this structure were refined with a constrained geometry. The aryl and the methyl H-atoms were included in structure factor computations in calculated positions, the methyls being treated as rigid groups. The hydroxyl hydrogen atoms in structure (3) were located directly in difference-Fourier maps. The final refinements were based on observations for which $F_o^2 > 3\sigma(F_o^2)$, using experimental weights $w = [\sigma^{-2}(F_o)]$ and minimizing $w(\Delta F)^2$. The final difference-Fourier maps showed no indication of incorrectly placed or missing atoms. The crystallographic labeling scheme used is shown below. Since the asymmetric unit of (2) consists of three independent molecules of the free ligand, atoms in the different species are marked by unprimed, primed and double primed labels, respectively (see Table II).



3. Results

Final atomic coordinates and equivalent isotropic temperature factors of (2) and (3) are listed in Tables II and III, respectively. Lists of the anisotropic thermal parameters, bond lengths and bond angles have been deposited.

In the diol host the two phenyl rings are characteristically twisted in an asymmetric manner with respect to the plane defined by the central C(1)—C(2)—C(3) fragment. Somewhat unexpectedly, the observed distances for the C(2)—C(aryl) bonds are consistently longer than those for the C(2)—C(methyl) bonds. Thus, in the three crystallographically independent molecules in (2) the formally C(sp³)—C(sp²) bond distances are within the range 1.56–1.57 Å, 1.54–1.56 Å and 1.57–1.57 Å, while the corresponding C(sp³)—C(sp³) bonds vary within 1.52–1.54 Å, 1.52–1.53 Å, and 1.53–1.55 Å. Similarly in (3), the two C(sp³)—C(sp²) bond lengths are 1.54 Å, while the C(sp³)—C(sp³) ones range from 1.52 to 1.53 Å. The excessive apparent stretching of the C—C bonds in (2) can be an artifact of the constrained refinement employed in this case.

The crystal structure of (2) is illustrated in Figure 1. It reflects the strong tendency of the —OH functional groups to act as proton donors and proton acceptors at the same time. Each OH associates strongly with two neighboring molecules, forming two-dimensional networks of hydrogen bonded species roughly parallel to the *ab* plane of the crystal. The 'head-to-tail' O(10)⋯O(17) type H-bonding distances between adjacent molecules displaced by $x = \pm 1$ along *a* are 2.81(1), 2.86(1) and 2.74(1) Å for the three independent moieties. The cross-linking bonds along the *b*-direction are O(10)⋯O(17') = 2.99(1) Å, O(17)⋯O(10'') = 2.67(1) Å, and O(10')⋯O(17'')(at $-0.5 - x, 0.5 + y, 0.5 - z$) = 2.84(1) Å (Figure 1b). The layered clusters are stacked one on top of the other along the *c* axis of the

Table I. Summary of crystal data and experimental parameters.

Compound	(2)	(3)	(4) ^a
Formula	C ₁₅ H ₁₆ O ₂	C ₁₅ H ₁₆ O ₂ ·C ₇ H ₈ O	C ₁₅ H ₁₆ O ₂ ·C ₇ H ₈ O
mol. wt.	228.29	336.43	336.43
space group	<i>P</i> 2 ₁ / <i>n</i>	<i>P</i> 2 ₁ / <i>c</i>	<i>P</i> 2 ₁ / <i>n</i>
<i>Z</i>	12	4	4
<i>a</i> Å	11.210(3)	6.239(5)	6.219(4)
<i>b</i> Å	18.967(3)	15.037(6)	28.337(21)
<i>c</i> Å	17.927(9)	20.205(7)	10.909(6)
β /deg	100.90(2)	97.75(4)	102.86(5)
<i>V</i> /Å ³	3742.9	1884.5	1874.2
<i>D_c</i> /Mg m ⁻³	1.215	1.186	1.192
crystal size/mm ³	0.2 × 0.3 × 0.3	0.3 × 0.3 × 0.5	0.3 × 0.6 × 0.7
<i>F</i> (000)	1464	720	720
μ /m ⁻¹	0.074	0.072	0.072
<i>N</i> (unique) > 0	4172	2220	1274
<i>N</i> (obs) ^b	1536	1169	342
<i>R</i>	0.076	0.058	—
<i>wR</i>	0.071	0.055	—
$ \Delta\rho _{\max}$ /eÅ ⁻³	0.31	0.40	—

^aThis structure has not been refined.

^bWith $F_0^2 > 3\sigma(F_0)^2$.

Table II. Atomic positional and isotropic thermal parameters of (2). U_{eq} is one third of the trace of the orthogonalized U_{ij} tensor. The phenyl rings were refined as geometrically constrained rigid hexagons; the e.s.d.s of the corresponding atomic coordinates (given in parentheses) are thus smaller than those related to coordinates of the other individually refined atoms.

atom	x/a	y/b	z/c	U_{eq}
C(1)	0.4007(10)	0.5978(6)	-0.2338(6)	0.051(4)
C(2)	0.4375(9)	0.6465(6)	-0.1645(6)	0.041(3)
C(3)	0.4386(10)	0.7222(6)	-0.1918(6)	0.052(3)
C(4)	0.3486(6)	0.6405(3)	-0.1074(3)	0.036(3)
C(5)	0.2324(6)	0.6132(3)	-0.1325(3)	0.049(4)
C(6)	0.1473(6)	0.6148(3)	-0.0849(3)	0.046(3)
C(7)	0.1784(6)	0.6438(3)	-0.0123(3)	0.040(3)
C(8)	0.2946(6)	0.6711(3)	0.0128(3)	0.046(4)
C(9)	0.3797(6)	0.6695(3)	-0.0348(3)	0.043(4)
O(10)	0.0935(6)	0.6465(4)	0.0329(4)	0.059(3)
C(11)	0.5652(7)	0.6196(3)	-0.1219(4)	0.038(3)
C(12)	0.6672(7)	0.6628(3)	-0.1165(4)	0.053(4)
C(13)	0.7789(7)	0.6405(3)	-0.0751(4)	0.052(4)
C(14)	0.7885(7)	0.5750(3)	-0.0390(4)	0.050(4)
C(15)	0.6864(7)	0.5319(3)	-0.0443(4)	0.052(4)
C(16)	0.5748(7)	0.5542(3)	-0.0858(4)	0.045(3)
O(17)	0.8944(6)	0.5535(4)	0.0069(4)	0.064(3)
C(1')	-0.3291(11)	0.8682(7)	-0.0790(7)	0.082(4)
C(2')	-0.2999(10)	0.9039(6)	-0.0017(6)	0.049(3)
C(3')	-0.2893(11)	0.9832(7)	-0.0150(8)	0.081(4)
C(4')	-0.4020(5)	0.8918(3)	0.0454(4)	0.035(3)
C(5')	-0.3856(5)	0.9212(3)	0.1179(4)	0.041(4)
C(6')	-0.4748(5)	0.9129(3)	0.1620(4)	0.042(3)
C(7')	-0.5803(5)	0.8751(3)	0.1335(4)	0.048(4)
C(8')	-0.5967(5)	0.8456(3)	0.0610(4)	0.053(4)
C(9')	-0.5076(5)	0.8540(3)	0.0169(4)	0.052(4)
O(10')	-0.6667(6)	0.8683(4)	0.1782(4)	0.056(3)
C(11')	-0.1818(6)	0.8695(3)	0.0406(3)	0.034(3)
C(12')	-0.0721(6)	0.9056(3)	0.0461(3)	0.038(3)
C(13')	0.0366(6)	0.8730(3)	0.0791(3)	0.049(3)
C(14')	0.0356(6)	0.8042(3)	0.1065(3)	0.039(3)
C(15')	-0.0741(6)	0.7680(3)	0.1009(3)	0.045(3)
C(16')	-0.1828(6)	0.8007(3)	0.0680(3)	0.046(4)
O(17')	0.1398(6)	0.7691(4)	0.1389(4)	0.057(3)
C(1'')	0.5787(11)	0.6719(6)	0.3874(6)	0.067(4)
C(2'')	0.5463(9)	0.6680(6)	0.3007(6)	0.042(3)
C(3'')	0.5258(11)	0.7437(6)	0.2688(7)	0.064(4)
C(4'')	0.6483(7)	0.6339(4)	0.2634(3)	0.039(3)
C(5'')	0.7604(7)	0.6142(4)	0.3064(3)	0.052(4)
C(6'')	0.8501(7)	0.5863(4)	0.2707(3)	0.060(4)
C(7'')	0.8277(7)	0.5779(4)	0.1920(3)	0.047(4)
C(8'')	0.7156(7)	0.5975(4)	0.1490(3)	0.060(3)
C(9'')	0.6259(7)	0.6255(4)	0.1847(3)	0.061(4)
O(10'')	0.9186(6)	0.5504(4)	0.1579(4)	0.062(3)
C(11'')	0.4287(5)	0.6220(4)	0.2784(4)	0.042(3)
C(12'')	0.4422(5)	0.5500(4)	0.2936(4)	0.053(4)
C(13'')	0.3427(5)	0.5050(4)	0.2746(4)	0.050(3)
C(14'')	0.2298(5)	0.5319(4)	0.2405(4)	0.052(4)
C(15'')	0.2163(5)	0.6039(4)	0.2253(4)	0.052(3)
C(16'')	0.3158(5)	0.6490(4)	0.2442(4)	0.052(4)
O(17'')	0.1321(6)	0.4863(4)	0.2227(4)	0.058(3)

Table III. Atomic positional and isotropic thermal parameters of (3). U_{eq} is one third of the trace of the orthogonalized U_{ij} tensor.

atom	x/a	y/b	z/c	U_{eq}
C(1)	0.4010(10)	0.3973(4)	0.1068(3)	0.063(2)
C(2)	0.1999(9)	0.4462(3)	0.1218(2)	0.041(2)
C(3)	0.0096(10)	0.4058(4)	0.0758(2)	0.063(2)
C(4)	0.1746(9)	0.4342(3)	0.1960(2)	0.039(2)
C(5)	-0.0077(9)	0.3995(4)	0.2178(2)	0.047(2)
C(6)	-0.0247(9)	0.3940(4)	0.2861(3)	0.049(2)
C(7)	0.1400(10)	0.4230(3)	0.3321(2)	0.041(2)
C(8)	0.3259(9)	0.4564(4)	0.3123(3)	0.048(2)
C(9)	0.3393(9)	0.4615(4)	0.2448(3)	0.047(2)
O(10)	0.1269(6)	0.4186(2)	0.4000(2)	0.051(1)
C(11)	0.2061(9)	0.5462(3)	0.1070(2)	0.038(2)
C(12)	0.0424(9)	0.6009(4)	0.1226(2)	0.045(2)
C(13)	0.0387(9)	0.6903(4)	0.1092(3)	0.048(2)
C(14)	0.2028(10)	0.7278(4)	0.0800(2)	0.043(2)
C(15)	0.3690(9)	0.6759(4)	0.0645(2)	0.041(2)
C(16)	0.3705(9)	0.5853(4)	0.0777(2)	0.040(2)
O(17)	0.1926(6)	0.8175(3)	0.0680(2)	0.055(1)
O(18)	0.4851(6)	0.3884(2)	0.4884(2)	0.056(1)
C(19)	0.4548(11)	0.3714(4)	0.5533(3)	0.046(2)
C(20)	0.2631(10)	0.3891(4)	0.5760(3)	0.057(2)
C(21)	0.2402(10)	0.3708(4)	0.6420(3)	0.058(2)
C(22)	0.4060(11)	0.3341(4)	0.6851(3)	0.052(2)
C(23)	0.5999(11)	0.3186(4)	0.6608(3)	0.060(2)
C(24)	0.6249(10)	0.3371(4)	0.5960(3)	0.052(2)
C(25)	0.3792(12)	0.3105(4)	0.7561(3)	0.087(2)
H(10)	-0.0101	0.3837	0.3973	0.050
H(17)	0.3264	0.8437	0.0541	0.050
H(18)	0.3491	0.4167	0.4581	0.050

unit cell, associating only weakly via dispersion between their hydrophobic surfaces. Presumably, the need to facilitate the interlayer van der Waals packing is the main reason for having three differently oriented molecules in the asymmetric unit of this structure.

The crystal structure of the 1:1 inclusion complex with *p*-cresol (3) is illustrated in Figure 2. It contains continuous chains of strongly H-bonded host species which extend along the *b*-direction. Adjacent chains displaced along *a* are now linked by the guest constituent; the latter donates its hydroxyl proton to one chain, while accepting another proton from the neighboring one. Consequently, this structure also consists of two-dimensional arrays of H-bonded entities which are stacked along the third dimension. The layered arrangement is, however, not as flat as in the previous example. Rather, the lipophilic surface consists of alternating concave and convex sections. There are no short contacts between adjacent guests displaced edge-to-edge along the *a* axis.

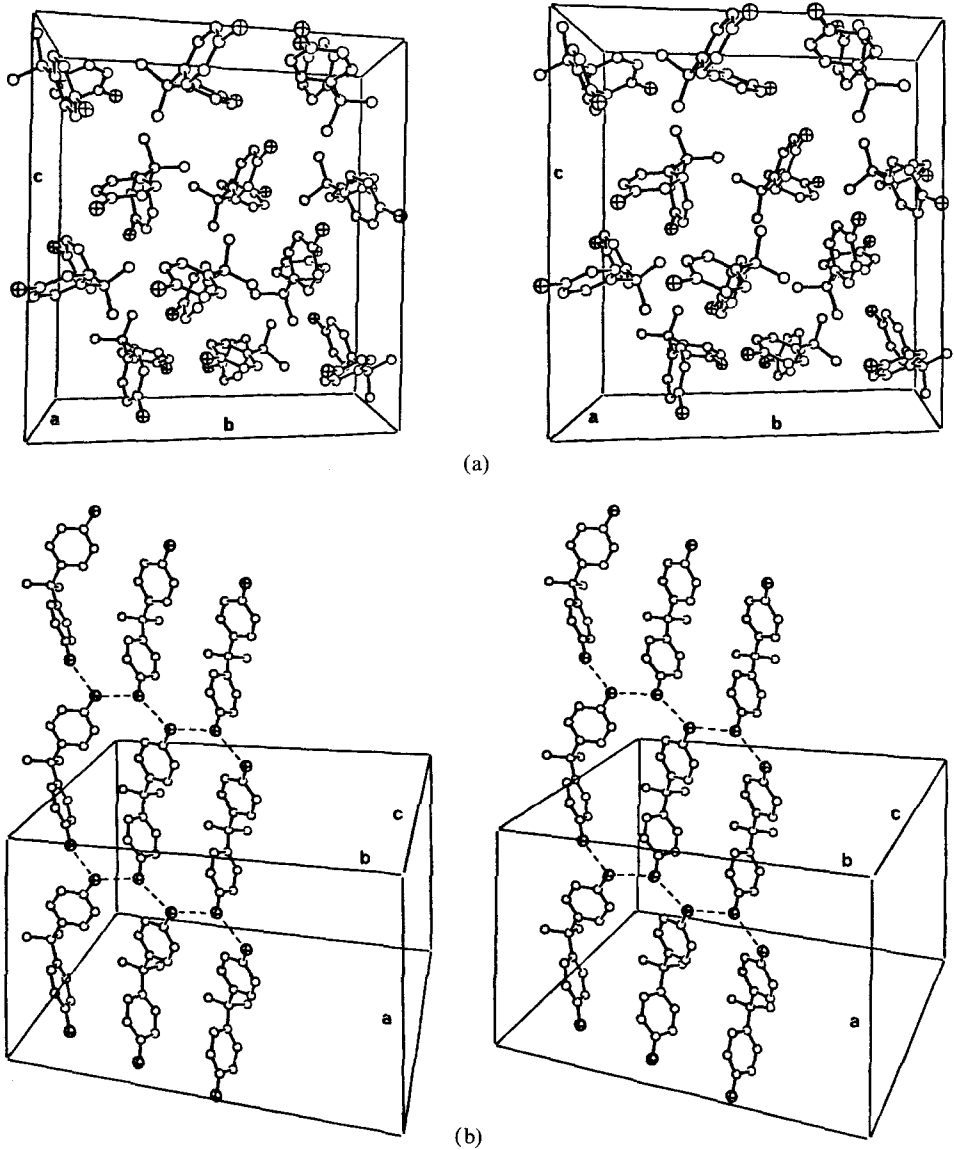
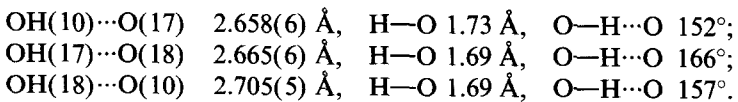


Fig. 1. Stereoviews of the crystal structure of 2,2-di(*p*-dihydroxyphenyl)propane, showing: (a) the contents of the unit cell, and (b) the H-bonding network parallel to the *ab* plane. The oxygen atoms are indicated by crossed circles.

The geometric parameters of host–host and host–guest hydrogen bonds in structure (3) are:



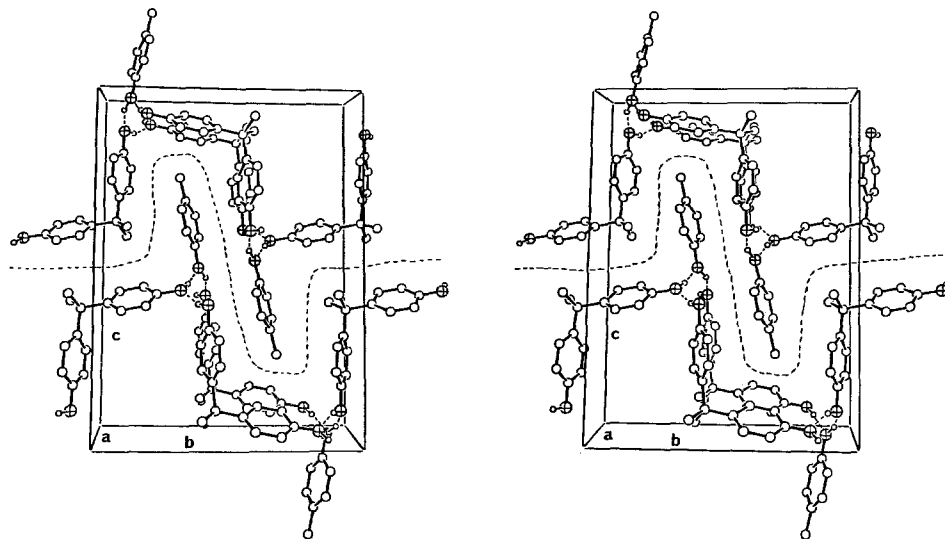


Fig. 2. Stereoview of the inclusion complex of (2) and *p*-cresol down the *a*-axis (*b* is horizontal). The wavy dashed line marks the lipophilic interface between adjacent layers of H-bonded molecules. Contents of more than one unit cell are shown in order to illustrate better the host–host and host–guest coordinations, as well as the convenient steric fit between the layers.

The crystal structure of the *m*-cresol complex (4) could not be analysed due to an insufficient amount of significant experimental observations. However, the unit cell and space group data indicate clearly that this crystal structure is isostructural to that found in the 1:1 complexes of host (1) with cyclohexanol and cyclohexanone (see below) [9]. Moreover, a trial refinement of a geometrically constrained structural model for the (2)·*m*-cresol complex, which was based on the (1)·cyclohexanol structure, with an overall isotropic thermal parameter and the small set of data led to a reasonably low *R* factor (17%); however, the results are obviously not precise and not entirely reliable.

4. Discussion

The solid structures of molecular compounds containing polar sites available for hydrogen bonding are determined primarily by optimization of the hydrogen bonds. The relative stability of the intermolecular arrangement in similarly structured or closely related compounds is then affected by weaker secondary interactions between the nonpolar fragments of the constituent molecules. This has been beautifully demonstrated in the preceding papers related to the selective inclusion behaviour of host (1) [8, 9]. All the studied inclusion complexes between (1) and phenolic derivatives (phenol, *o*-cresol, *m*-cresol and *p*-cresol), or cyclohexanol, form similar types of structure with an identical two-dimensional pattern of intermolecular hydrogen bonds (Figure 3). Along one dimension of the H-bonded arrays, adjacent host molecules displaced by 10.85 ± 0.04 Å are bound to each other directly through their terminal —OH functions. The various guests in the respective

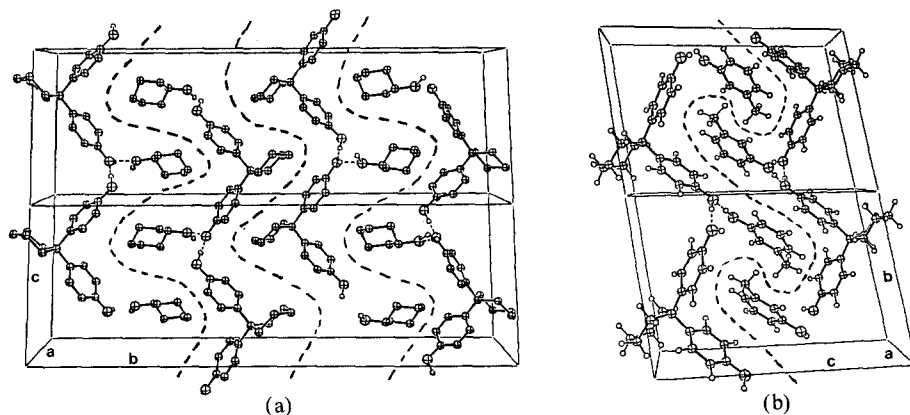


Fig. 3. Crystal structures of 1:1 complexes between 1,1-di(*p*-dihydroxyphenyl)cyclohexane and: (a) cyclohexanol, and (b) *m*-cresol viewed down the short 6.2 Å axis, showing the intermolecular coordination and packing modes. The wavy dashed lines indicate van der Waals interfaces between the hydrogen bonded networks (taken from Refs. [8] and [9]).

complexes bridge between the hosts in the other direction, the translation vector of which is also fixed at 6.25 ± 0.02 Å. The interlayer packing along the third axis of the crystal is stabilized by weaker forces, being therefore most sensitive to structural modification. In complexes with the aromatic guests two such layers are contained in a triclinic unit cell, the length of the crystallographic translation increasing from 14.85 Å in the phenol complex, through 15.45–15.49 Å in the *o*-cresol and *m*-cresol compounds, to 15.82 Å for the *p*-cresol adduct [8]. The steric fit between consecutive layers is more complementary, however, in the *m*-cresol case than in the other structures, giving rise to preferential co-crystallization of (1) with this guest [8]. In the cyclohexanol complex the respective dimension of the unit cell is about twice as large (32.22 Å), extending over four H-bonded layers rather than two [9]. There are two different interlayer surfaces in this structure-type. Along one, the nonbonding interactions are between guest/guest and host/guest components; along the other surface only the host molecules interact with one another (mainly) through their cyclohexyl rings. Interchanging between the different guests affects, therefore, primarily, one interface between the layers. The design of host (2) represents an attempt to modify the second interface as well.

Co-crystallization of host (2) with various alcoholic species indicates that the aromatic guest component contributes favourably to the stabilization energy of the solid phase by a better optimization of the dispersive interactions (at least in the complex with *p*-cresol), and/or by an increased entropy. Significant enthalpic contribution of weakly polar interactions between aromatic rings has recently been estimated quantitatively for protein structures [13].

The 1:1 complex of host (2) with *m*-cresol forms, undoubtedly, the same structure type as described above and in Figure 3a. The translation vectors in the *ac* plane of 6.22 and 10.91 Å (Table I) are perfectly compatible with the previously observed data [8, 9], indicating that the two dimensional network of hydrogen bonding is maintained as before. Moreover, the interlayer packing along the third

direction in (4) is comparable to that found in the complex of (1) with cyclohexanol [9], the length of the *b* axis decreasing from 32.22 Å in the latter to 28.34 Å in the former due to the replacement of the cyclohexyl ring by the smaller propyl moiety (the relevant net diameter of the excluded three-carbon atom fragment is indeed about 2 Å). The decreased size of the hydrocarbon surface of host (2), as compared to (1), has a significant effect on the overall stability of the structure, causing less favorable dispersion interaction along the 'host only' interface between the neighboring layers (see above). As a result, the crystals of (4) are less stable, and diffract poorly. A consistent indication is provided by the melting points of the relevant solids of (1)·*m*-cresol, (1)·cyclohexanol and (2)·*m*-cresol which are 157–159, 140–142 and only 91–92°C, respectively. In this type of intermolecular arrangement, complexes of (2) with the phenol and *o*-cresol moieties are expected to be even less stable [8].

Evidently, the higher selectivity of (2) for *p*-cresol is associated with modification of the crystal packing. In the previously described set of structures [8, 9], along any given chain of H-bonded hosts the convex surfaces of all molecules are aligned in the same direction (... ^ ^ ^ ...). On the other hand, in the present *p*-cresol adduct with (2), H-bonded chains are formed between hosts with alternating orientations (... ▽ ▽ ▽ ...). Such an arrangement allows for a considerably larger area of contact between the lipophilic surfaces of adjacent H-bonded layers. Figure 2 shows that the square-wave type chains of the diol molecules are linked to one another through the *p*-cresol guest in the same manner as in other complexes, the periodic displacement along this direction remaining at 6.24 Å. The van der Waals interface between the H-bonded shells of host molecules in this structure is now perfectly suited to accommodate the *p*-cresol entity (the hydrocarbon part of the latter being effectively surrounded by the aryl groups of the host species), with an optimal steric fit between neighboring shells. However, all layers are now crystallographically equivalent, and the hosts of adjacent layers are in close contact with one another around $y = 0.0$ and $y = 1.0$ along the unique interface (Figure 2). A similar packing arrangement with the *m*-cresol guest cannot be stable. A more condensed stacking of the H-bonded layers along *c*, which is required to compensate for the alternative substitution of the guest methyl (as formerly observed in the inclusion adducts of (1) [8]), would be severely hindered in this structure-type. The selective complexation of (2) with *p*-cresol from its mixtures with other phenols should thus be attributed to the formation of the unique crystalline phase.

The present results demonstrate that coordination assisted complexation can effectively be used for separations between closely related structural isomers, and that it is possible to adapt a suitable host for a particular application by a small structural variation of its molecular framework. The 'breathing' ability of the crystal lattice is considerably limited by the strong hydrogen bonding features, increasing the significance of secondary interactions [13] and enhancing preferential accommodation of guests better shaped to fit into the particular structure type. Further exploration of molecular recognition patterns of hosts containing other binding groups should, undoubtedly, lead to additional interesting applications. Encouraging results have already been reported for the carboxylic acid and amide derivatives [14, 15].

Acknowledgements

I.G. is grateful to the Department of Chemistry and Biochemistry at UCLA for the hospitality extended to him while working on this manuscript during a sabbatical stay at UCLA.

References

1. *Inclusion Compounds*, vols. I-III, J. L. Atwood, J. E. D. Davies, and D. D. MacNicol (eds.), Academic Press, London (1984).
2. *Molecular Inclusion and Molecular Recognition – Clathrates I and II*, E. Weber (ed.), *Topics in Current Chemistry*, vols. 140 and 149, Springer, Berlin (1987 and 1988).
3. F. Toda: in ref. 2, vol. 140, p. 43 (1987).
4. K. Mori, and F. Toda: *Chem. Lett.* 1988, 1997; F. Toda, and K. Mori: *J. Chem. Soc., Chem. Commun.* 1986, 1357; T. Fujiwara, N. Tanaka, R. Ooshita, R. Hino, K. Mori, and F. Toda: *Bull. Chem. Soc. Jpn.* **63**, 249 (1990).
5. F. Toda, K. Mori, Z. Stein, and I. Goldberg: *J. Org. Chem.* **53**, 308 (1988) and *Tetrahedron Lett.* **30**, 1841 (1989).
6. F. Toda, and K. Tanaka: *Tetrahedron Lett.* **29**, 1807 (1988); G. H. Lee, Y. Wang, K. Tanaka, and F. Toda: *Chem. Lett.* 1988, 781.
7. F. Toda, and K. Tanaka: *Tetrahedron Lett.* **29**, 551 (1988).
8. I. Goldberg, Z. Stein, K. Tanaka, and F. Toda: *J. Incl. Phenom.* **6**, 15 (1988).
9. I. Goldberg, Z. Stein, A. Kai, and F. Toda: *Chem. Lett.* 1987, 1617.
10. F. Toda, K. Tanaka, T. Hyoda, and T. C. W. Mak: *Chem. Lett.* 1988, 107.
11. G. M. Sheldrick: SHELXS-86. In *Crystallographic Computing 3*, G. M. Sheldrick, C. Kruger, and R. Goddard (eds.), Oxford University Press pp. 175–189 (1985).
12. G. M. Sheldrick: SHELX-76. Program for Crystal Structure Determination, University of Cambridge, England (1976).
13. S. K. Burley, and G. A. Petsko: *J. Am. Chem. Soc.* **108**, 7995 (1986) and *Science* **229**, 23 (1985).
14. E. Weber, I. Csöreg, B. Stensland, and M. Czugler: *J. Am. Chem. Soc.* **106**, 3297 (1984); E. Weber, I. Csöreg, J. Ahrendt, S. Finge, and M. Czugler: *J. Org. Chem.* **53**, 5831 (1988).
15. I. Goldberg, L. T. W. Lin, and H. Hart: *J. Incl. Phenom.* **2**, 377 (1984); H. Hart, L. T. W. Lin, and I. Goldberg: *Mol. Cryst. Liq. Cryst.* **137**, 277 (1986).